MODELLING SHALLOW HEAT TRANSFER AT KARAPITI

J.A.NEWSON[1], M.J.O'SULLIVAN[1], C. J. BROMLEY[2], AND M. P. HOCHSTEIN[1]

[1] University of Auckland, Auckland, New Zealand

[2] Institute of Geological and Nuclear Sciences, Taupo, New Zealand

SUMMARY – Temperature measurements in shallow soils together with three simple heat flow models are used to derive the apparent thermal diffusivity, and to identify heat and mass flows.

1. INTRODUCTION

Shallow ground temperatures have been recorded at 5 sites around the Karapiti Thermal Area, Wairakei, New Zealand Bromley & Hochstein, (in press). Temperatures were recorded at the surface, and at various depths at each site. In the present study these data are used with three simple heat flow models to determine the thermal diffusivity values for the Karapiti sites, and to investigate the shallow subsurface heat and mass transfer processes.

Three mathematical models are used in this study. The first (the simple conductive model), is based on an analytic solution of the one-dimensional heat conduction equation. The temperature at the upper boundary is represented by a sinusoidal function, which is provided by a Fourier analysis of the field data. The model simplifies the field situation by treating the soil as a uniform, semi-infinite layer. A similar approach was reported by Carson, (1963), Dawson & Fisher, (1964), and Hurley & Wiltshire, (1993).

The second model also allows heat transfer by conduction, but at the surface a more complex heat-loss boundary condition model is used. This allows the air temperature to be different to the surface temperature. In the third model mass flow is allowed giving advective/conductive heat transfer in the soil.

The apparent thermal diffusivity determined for three of the four sites considered (KP02, KP03, KP04) has a range of values in close agreement with Dawson & Fisher, (1964). Another site (KP01) shows evidence of cyclic heat input from depth.

2. MATHEMATICAL MODELS

The fundamental problem to be solved is: given the atmospheric temperature, $T_a(t)$, and the temperature measured at various depths, $T(z,t)$, determine the thermal diffusivity κ of the shallow region of the geothermal system. In order to solve this problem the following three idealised mathematical models were considered.

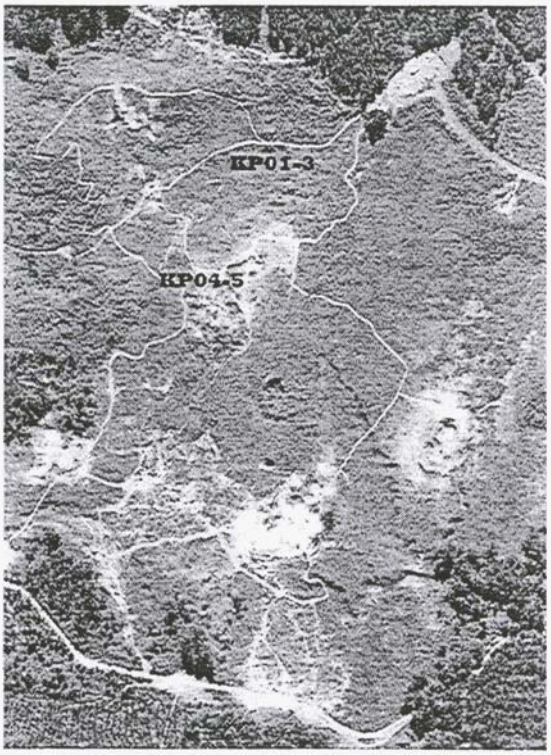

Figure 1. Aerial photo of Karapiti Thermal Area, showing approximate data collection points.

I. Simple conductive model

$$\frac{\partial T}{\partial t} = \kappa \frac{\partial^2 T}{\partial z^2} \quad \text{for } 0 < z < \infty \tag{1}$$

$$T(0,t) = T_a(t) \tag{2}$$

$$q(z,t) \to -q_d \quad \text{as } z \to \infty \tag{3}$$

Here $q(z,t)$ is the heat flux defined by

$$q = -k \frac{\partial T}{\partial z} \tag{4}$$

where k is the conductivity.

II. Heat-loss surface conditions

The same differential equation (1) is used but the heat loss at the surface is proportional to the

difference between the surface temperature (T(0,t) and the air temperature ($T_a(t)$). Hence the surface boundary condition **(2)** is replaced by

$$-k\frac{\partial T}{\partial z}(0,t)=h(T(0,t)-T_a(t)) \qquad (5)$$

In the case where the surface heat transfer h is very large, (5) reduces to (2).

111. Mass through-flow

In this case the differential equation is

$$\frac{\partial T}{\partial t}-V\frac{\partial T}{\partial z}=\kappa\frac{\partial^2 T}{\partial z^2} \qquad (6)$$

Here V is defined in terms of the mass flux q_m by

$$V=\frac{c_f q_m}{(\rho c)_{eff}} \qquad (7)$$

and

$$(\rho c)_{eff}=\rho_f c_f \phi+\rho_r c_r(1-\phi) \qquad (8)$$

The diffusivity κ in (1) or (6) is defined by

$$\kappa=\frac{k}{(\rho c)_{eff}} \qquad (9)$$

Equation (7) is valid for single phase flow only (water or steam). For the sign convention used here V is positive for upwards flow and negative for downwards flow.

2.1 Surface temperature

The air temperature has a strong periodic component and therefore it is appropriate to approximate air temperature by a finite Fourier series of the form

$$T_a(t)=C_0+\sum_{n=1}^{N}C_n\cos(\omega_n t-\varphi_n) \qquad (10)$$

Here

$$\omega_n=\frac{2\pi n}{\tau} \qquad (11)$$

where τ is the total length of time in the record. For the data considered τ = 72, 96, or *144* hrs. The dominant term in (10), is the diurnal term, corresponding to n=3, 4, or 6.

The steady component in the temperature arising from the C_0 term and the main diurnal periodic component are considered separately. This results in two simple representations of $T_a(t)$ for models I, 11 and III, namely:

(i) $T_a(t)=C_0$ (12)

(ii) $T_a(t)=C_n\cos(\omega_n t-\varphi_n)$ (13)

The following solutions were obtained for (i)

Table 1. Solutions for mean temperature

Problem	Solution	Parameter values
I	$T=A_0+B_0 z$	$A0=C_0$ $B_0=\frac{q_d}{k}$
II	$T=A_0+B_0 z$	$A_0=C_0+\frac{q_d}{h}$ $B_0=\frac{q_d}{k}$
III	$T=A_0+B_0 e^{-\eta z}$	$A_0=T_d$ $B_0=C_0-T_d$ $\eta=\frac{V}{\kappa}$

Note that T_d is the temperature of the deep upflow and the deep heat flux is given by

$$q_d=c_f q_m T_d \qquad (14)$$

For the boundary condition (ii) the solution for all three problems can be written in the form

$$T=\lambda C_n e^{-\beta z}\cos(\omega_n t-\gamma z-\varphi_n-\varepsilon) \qquad (15)$$

The parameters in *(15)* are given in Table 2.

Table 2. Parameters in equation (15)

Problem	Parameters
I	$\lambda=1,\ \beta=\frac{a}{\sqrt{2}},\ \gamma=\frac{a}{\sqrt{2}}$ $\varepsilon=0,\ a=\sqrt{\frac{\omega}{\kappa}}$
II	$\lambda=\frac{1}{\delta},\ \beta=\frac{a}{\sqrt{2}},\ \gamma=\frac{a}{\sqrt{2}}$ $\varepsilon=\tan^{-1}\left(\frac{b}{1+b}\right),\ b=\frac{ka}{h\sqrt{2}}$ $\delta=\sqrt{b^2+(1+b)^2}$
III	$\lambda=1,$ $\beta=\sqrt{r}\left(\cos\frac{\theta}{2}+\sqrt{\cos\theta}\right)$ $\gamma=\sqrt{r}\sin\frac{\theta}{2},\ \varepsilon=0,\ r=\sqrt{a^4+d^4}$ $d=\frac{V}{2\kappa},\ \theta=\tan^{-1}\left(\frac{a^2}{d^2}\right)$

Equation (15) can be re-written as

$$T(z,t) = C_n^*(z)\cos\left(\omega_n t - \varphi_n^*(z) - \varphi_n\right) \qquad (16)$$

here

$$\frac{C_n^*(z)}{C_n} = \lambda e^{-\beta z} \qquad (17)$$

and

$$\varphi_n^*(z) = \gamma z + \varepsilon \qquad (18)$$

Taking the log of (17) gives

$$\ln\left(\frac{C_n^*(z)}{C_n}\right) = -\beta z + \ln\lambda \qquad (19)$$

Thus for all three models plots of φ_n^* vs z and $\ln\left(C_n^*/C_n\right)$ vs z both give straight lines with slopes y and $-\beta$ respectively.

2.2 Model features

Model I is the one most commonly used to derive thermal diffusivity, for example by Dawson & Fisher, (1964), Carson, (1963), Hurley & Wiltshire, (1993).

Note that for models I and II, $\gamma = \beta$ and both plots should have the same slope (in magnitude). For models I and III, $\lambda = 1$ and $\varepsilon = 0$, so both plots should have a zero intercept. The plots of mean temperature are linear for models I and II, and exponential for III.

Obviously many other more complex models are possible. For example, the authors have carried out preliminary studies on two-layer models, and are also investigating general nonhomogeneous models using the TOUGH2 geothermal simulator.

3. DATA DESCRIPTION

Temperature measurements were taken over periods of 4 to 8 days, at 5 sites around Karapiti. The sites are KP01, KP02, KP03, KP04, and KP05.

Temperatures were recorded at the surface, and depths of 1 cm, 5 cm, 10 cm, 15 cm, and 20 cm. Soil samples were also taken at 0 – 15 cm and 15 – 30 cm depth for laboratory analysis of moisture content and density determinations. (see Bromley & Hochstein, (in press)). Some subsets of the data were analysed separately, and there are 7 analyses reported from 4 sites. KPOl data (Figure 2) shows non-periodic behaviour for the first 24 hours, and a separate analysis has been applied to the period from 24 to 96 hours; this data subset is called KP01_72. Repeat measurements at the same site are called KP01a (Figure 3). This data shows the effects of rainfall suppressing the diurnal temperature variation for the last two days of measurement. Therefore there is also a separate analysis of the 96 hr period before the rainfall. This data set is called KP01a_96. Data from the remaining sites are referred to by the site name: KP02, KP03, and KP04 (Figure 4, Figure 5, and Figure 6). The data from site KP05 lacks the periodicity required for a Fourier analysis.

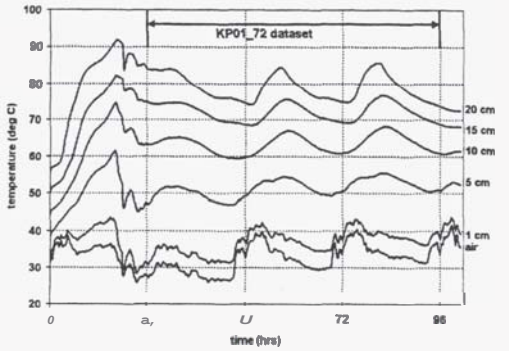

Figure 2. KP01: measured temperatures.

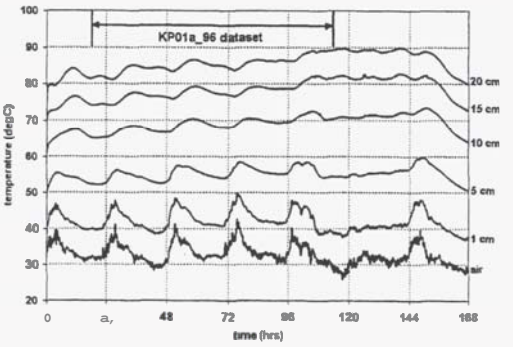

Figure 3. KP01a: measured temperatures.

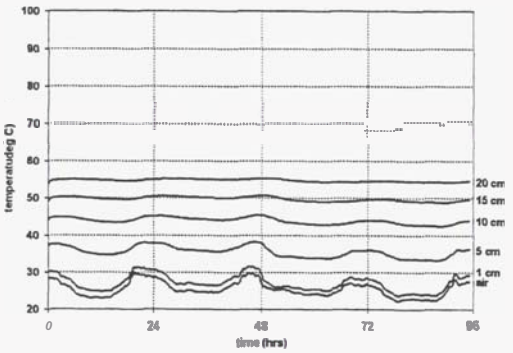

Figure 4. KP02: measured temperatures.

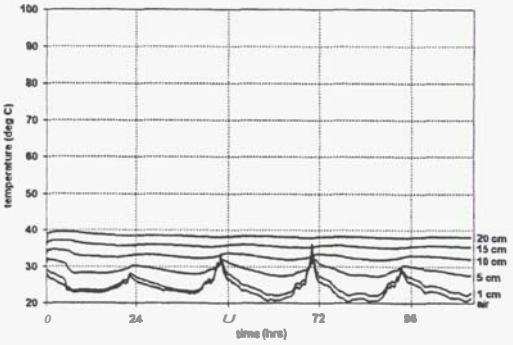

Figure 5. KP03: measured temperatures.

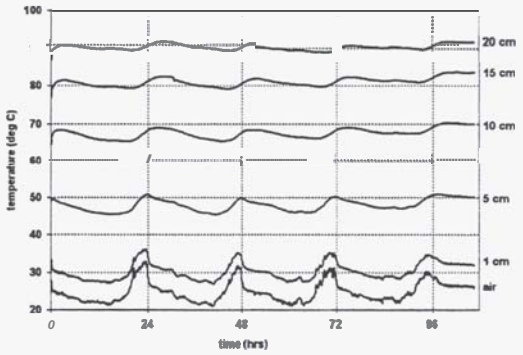

Figure 6. KP04: measured temperatures.

4. RESULTS

4.1 Fourier Analysis

The near-surface temperature measured over 4 to 6 days at the Karapiti sites show the strong influence of daily temperature cycle, but also show the influence of non-periodic factors such as cloud cover, rain, barometric pressure, and steam flow. The diurnal components in the data are isolated by Fourier analysis, as described in (10) and (11). The analysis provides the amplitude of the each cycle (C), and the time of the temperature peak (the phase shift (φ)), at each depth. Equations (17) and (18) give the theoretical relationship of the variation of amplitude with depth, and the phase shift with depth, respectively.

Similarly the results in Table 1 enable the measured mean temperatures to be used to deduce the heat flux from depth q_d and related parameters.

A Fourier analysis of the Karapiti data shows that, as expected, the diurnal term is dominant in all cases. The C_0 term in the Fourier series can be used to produce a plot of the mean temperature versus depth (Figure 7) without the imposed periodic fluctuations. For a uniform soil and with no mass flow this plot should be linear. The varying temperature gradients with depth in Figure 7 are evidence for:

(i) a layered soil structure,

(ii) variation in porosity or liquid saturation, or

(iii) a through flow of mass

or all three of these effects.

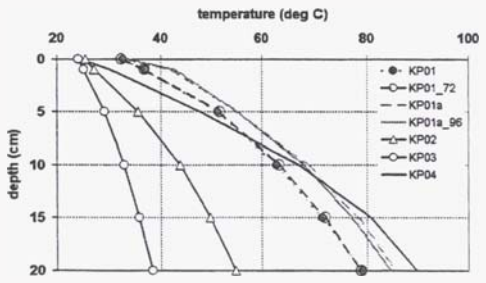

Figure 7. Mean temperature (θ_m) versus depth for each dataset.

The relatively high surface temperatures for four KP01 data sets suggest that model II with the heat loss surface condition might be appropriate for these cases. However consideration of the diurnal component for these data sets (see below) shows that none of the models considered here fit these data.

Figure 8 and Figure 9 show the diurnal amplitude and phase angle versus depth, respectively. Surface effects, (for instance, solar radiation and vegetation) can be seen in the temperature amplitude at 1 cm (Figure 8).

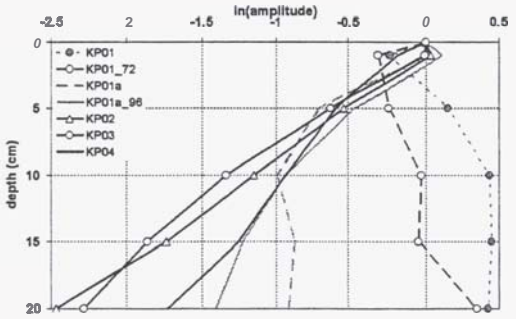

Figure 8. Amplitude versus depth of the diurnal temperature variation (all datasets).

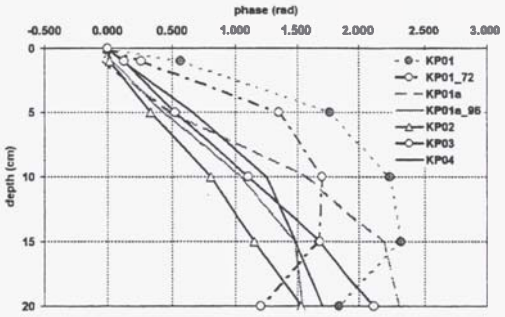

Figure 9. Phase angle versus depth of the diurnal temperature variation (all datasets).

KP01, KP01_72, and KP01a show temperature amplitude increasing with depth (Figure 8) and a reversal of the phase angle with depth (Figure 9). The effect is diminished when the rain-affected data are removed (KP01a_96) although neither the log of amplitude nor the phase shift are linear functions of depth.

The plot of logarithm of the amplitude, and of the phase shift, for KP02, KP03, and KP04 are approximately linear, and a best fit line through each set of data gives a value for β and γ.

4.2 Model results

Model I.

By inspection the mean temperature data for KP02, KP03 and KP04 (see Figure 7) can be matched approximately by Model I, and values of q_d/k (Table 1) calculated by fitting straight-lines to the data. Similarly the data for these three sites, shown in Figures 8 and 9, can be used to obtain

values of β and γ for Model I. A summary of the results obtained are shown in Table 3.

Table 3. Results for Model I

Data	KP02	KP03	KP04
q_d^*	149.2	72.3	332.7
β	12.52	11.99	8.20
γ	7.87	10.72	8.79
κ_{amp}	2.32E-7	2.53E-7	5.41E-7
κ_{phase}	5.87E-7	3.16E-7	4.71E-7

* assuming a value of 1W.m/K for k

The heat fluxes indicated by the values for q_d in Table 3 are high (at least 72.3-332.7W/m^2). The results for apparent thermal diffusivity are shown in Figure 10 together with results from Dawson & Fisher, (1964) for pumice soils at Wairakei, included for comparison.

Model II.

The results for KPOl in Figure 7 with the elevated surface temperatures suggest that Model II should be applied to these data sets. However the plots of in Figures 8 and 9 are not in agreement with (18) and (19) and therefore no further fitting of Model 11 was carried out.

Model III.

The data from KP02, KP03 and KP04 was used again to calibrate Model III. First the formula in Table 1 was matched, using nonlinear least squares giving the values for η and T_d shown in Table 4. The quality of the fit of the formula in Table 1 to the data in Figure 7 is excellent. Next the data from Figure 8 and Figure 9 was used to fit β and γ, and then from those parameters the value of a was calculated using the formulae in. Table 2. Finally the diffusivity was calculated. Unfortunately the values of diffusivity obtained using the amplitude data and the phase data differ (see Table 4). These results are also shown in Figure 10.

Table 4. Results for Model III

Data	KPO2	KPO3	KPO4
η =2d	4.80	4.63	5.86
T_d	72.9	47.7	119.7
β	12.52	11.99	8.20
γ	7.87	10.72	8.79
a_{amp}	14.1	13.5	6.8
a_{phase}	11.4	15.4	12.8
κ_{amp}	3.66E-7	3.99E-7	1.57E-7
κ_{phase}	5.60E-7	3.07E-7	4.44E-7

It was hoped that by using Model III, which fits the mean temperatures very well, more consistency between the two estimates of diffusivity would be obtained. However this is not the case and it is clear that the simple models investigated here are of limited usefulness for matching the measured data.

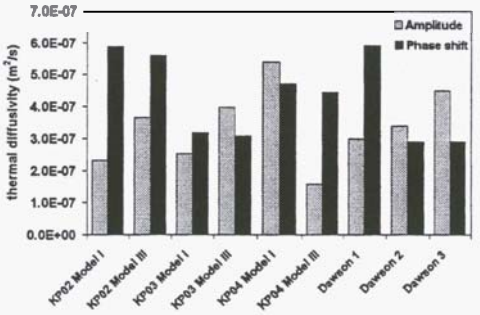

Figure 10. Thermal diffusivity for pumice soils, calculated fiom models I and III. Values from Dawson and Fisher (1964) for comparison. Dawson- 1 are values fiom the diurnal signal, Dawson 2 and 3 from the annual signals at a shaded site, and an exposed site, respectively.

5. DISCUSSION

5.1 Factors influencing the thermal regime

Model I and Model III

The models considered here are of limited accuracy because they assume that the soil is homogeneous and the flow is single phase. In fact neither of these assumptions are really valid.

Moisture content and soil type

Thermal diffusivity is dependent on the moisture content, and soil type. Field and laboratory evidence suggests that there is some variation in soil type and moisture content between sites. Hence some variation in thermal diffusivity is to be expected.

Layered structure

Soils generally have easily identifiable layers, which may have differing thermal properties; in addition, the existence of zones of condensation or evaporation may create a layered thermal structure in the soil. The models presented in this paper do not include the possibility of layering in the soil.

Variations in time

The Karapiti data presented here has been collected during relatively stable climatic conditions, and the analysis presented here assumes that soil parameters do not vary with time, and that the diurnal temperature cycle is a stable cycle.

Heat transfer processes in geothermal soils

Conduction is an important heat transport mechanism in soil, and is the sole means of heat

transport in Model I. Model 111 also includes advective heat transport, but only for a single phase fluid. It is likely that phase changes are also important at shallow depths in a geothermal soil.

Geothermal soils may also experience episodic or periodic heat input from the subsurface. The data for KP01 in Figure 8 with an increasing amplitude with depth suggests that a diurnal pulse of heat from depth may occur.

5.2 KP02, KP03, and KP04

Only data from KP02, KP03, and KP04 is used for thermal diffusivity calculations. Thermal diffusivity for these sites is between 0.16E-6 and 0.59E-6 m^2/s. This is similar to the range of 0.29E-6 to 0.59E-6 m^2/s reported by Dawson & Fisher, (1964).

Some difference between sites is expected, but the difference between K_{amp} and K_{phase} for the same site indicates that, although the models provide a reasonable estimate of thermal diffusivity, they not describing all the thermal processes.

5.3 KP01, and subsets of KP01 data

The increase in amplitude of the diurnal signal with depth, and the phase reversal means that another periodic heat input from depth must be occurring. For these sets of data the fit of the model formulae to the data is very poor and corresponding thermal diffusivity derived from amplitude and phase plots will be inaccurate. The simple models are not adequately describing the heat transfer processes, or the heat input, at the site.

6. CONCLUSIONS

The aim of modelling is to provide information about the physical processes occurring in the soil. In order to achieve this simple models have been used to represent processes that are considered to be important in the shallow subsurface. This approach has shown that models involving heat conduction, and mass transport (and advective heat transport) of a single phase fluid through a homogeneous soil layer give reasonable results but there are other processes which affect soil temperatures.

These studies have provided the basic conceptual models which are being used for developing more complex numerical models capable of including phase changes, layered soil structures, and a range of boundary conditions.

7. REFERENCES

Bromley, C. J. & Hochstein, M. P. (in press). Thermal properties of Steaming Ground, (Wairakei, New Zealand. *23rd New Zealand Geothermal Workshop,* University of Auckland.

Carson, J. E. (1963). Analysis of Soil and Air Temperatures by Fourier Techniques. *Journal of Geophysical Research,* 68(8), 2217-2232.

Dawson, G. B. & Fisher, R. G. (1964). Diurnal and Seasonal ground temperature variations at Wairakei. *New Zealand Journal of Geology and Geophysics,* 7, 144-154.

Hurley, S. & Wiltshire, R. J. (1993). Computing Thermal Diffusivity from Soil Temperature Measurements. *Computers and Geosciences,* 19(3), 475-477.